Water Science & Technology

Water Science & Technology Vol 90 No 4, 1198 doi: 10.2166/wst.2024.241

Cation interception and permeability characteristics of bentonite barriers exposed to NaCl and NH_4Cl solutions

Wen-jing Sun[a,b,*], Qian-tong Tang[a], Ri-dong Fan[a], Ai-wu Yang[a], Yun-zi Tan[c] and A. K. Leung[d]

[a] College of Environmental Science and Engineering, Donghua University, Shanghai 201620, China
[b] Key Laboratory of Ministry of Education on Safe Mining of Deep Metal Mines, Northeastern University, Shenyang 110819, China
[c] College of Civil Engineering and Architecture, China Three Gorges University, Yichang 443002, China
[d] Department of Civil and Environmental Engineering, Hong Kong University of Science and Technology, Clear Water Bay, Kowloon, Hong Kong, China
*Corresponding author. E-mail: wjsun@dhu.edu.cn

ABSTRACT

High concentrations of Na^+ and NH_4^+ in landfill leachate lead to deterioration of bentonite barrier and pose a threat to the environment. This study focused on the pollution interception and permeability characteristics of the bentonite barrier exposed to NaCl and NH_4Cl solutions. Based on previous findings, salt solution concentrations were established at 74.80, 37.40, 18.70, and 9.4 mmol/L. The bentonite contents in the mixture were set at 0, 5, 10, and 15%. The results indicate that the samples exhibit better interception of NH_4^+ compared to Na^+. This difference arises from the cation exchange sequence, the size of the hydration radius, and the hydrogen bonding of the two cations. Additionally, the difference in hydration enthalpy between the two cations leads to variations in the swelling of bentonite, resulting in a higher hydraulic conductivity coefficient in NH_4Cl solution. This study shows that although bentonite barriers have better interception for NH_4^+, they exhibit greater hydraulic conductivity in NH_4Cl solution, increasing the risk of leachate carrying other contaminants.

Key words: bentonite, cation exchange, cation interception, permeability characteristics, swelling index

HIGHLIGHTS

- Compared permeability and residual leachate of bentonite barriers in NaCl and NH_4Cl solutions.
- Bentonite intercepts NH_4^+ more effectively than Na^+.
- In NH_4Cl, bentonite has lower swelling and higher hydraulic conductivity than in NaCl.
- Variations in cation exchange, hydration radius, and bonding explain the differences.
- Hydration enthalpy differences lead to varying hydraulic conductivities in the solutions.

1. INTRODUCTION

Currently, urban solid waste management heavily relies on landfilling to dispose of solid wastes that cannot be recycled or incinerated. In China, approximately 79% of urban solid waste is disposed of in landfills (Havukainen *et al.* 2017).

High volume of leachate will be produced due to complex physical and chemical reactions during landfill operation. Na^+ and NH_4^+ constitute significant inorganic components, often present in high concentrations (Costa *et al.* 2019; Luo *et al.* 2020). It was found that NH_4^+ in leachate increased over time, and the concentration can be 2,000 mg/L (Negi *et al.* 2020). Within 1–2 years of operation in a landfill, the concentration of NH_4^+ can reach up to 4,000 mg/L (Sun *et al.* 2021). According to survey statistics, the average concentration of Na^+ in leachate is higher than that of common inorganic components such as K^+ and Ca^{2+} (averaging 1,675 and 400 mg/L, respectively), as well as other heavy metals (Cu^{2+}, Zn^{2+}, Pb^{2+}, etc.). The highest concentration approaches 4,000 mg/L (3,710 mg/L) (Naveen *et al.* 2017). As a result, leachate resulting from MSW landfills is a typical source of excessive NH_4^+ and Na^+, and these should be main cations considered for landfill design. Na^+ and NH_4^+ have little effect on bentonite engineering properties in low concentrations (80 mM) (Setz *et al.* 2017), but high value will affect the performance of bentonite barriers such as its morphological structure, swelling index (SI), hydraulic conductivity, and pollution interception (Anh *et al.* 2017; Setz *et al.* 2017). It may even affect the acidity and alkalinity of the environment (Lai *et al.* 2023).

Geosynthetic clay liners (GCLs) are often used in landfills to prevent the migration of potential pollution due to landfill leachate (Özçoban *et al.* 2022). However, both Na^+ and NH_4^+ are monovalent cations. Generally, in comparison to divalent cations, monovalent cations possess larger diffusion coefficients (Tadimeti & Chattopadhyay 2016; Huang *et al.* 2017; Aryal & Ganesan 2018; Dong *et al.* 2020). This facilitates their movement within the landfill liner. Further investigation is warranted to elucidate the variance in pollution interception capacity of bentonite for Na^+ and NH_4^+ present in landfill leachate. Additionally, the impact of Na^+ and NH_4^+ on the permeability properties of bentonite-based engineering barriers remains a subject that requires deeper scrutiny. Clarifying the distinctions in their respective influences is imperative. This study contributes to a better understanding of the behavior of leachate pollutants within landfill barriers, particularly focusing on the Na^+ and NH_4^+ retention in bentonite and the permeability alterations of bentonite.

To this end, mixture soil samples are prepared using bentonite and clay in this study, and the contents of bentonite are set at 0, 5, 10, 15, 20%, respectively. NaCl and NH_4Cl solutions with four different concentrations were used to permeate bentonite–clay mixture samples under a constant pressure. The leachate concentration of Na^+ and NH_4^+ was obtained. Fourier transform infrared (FTIR) analysis was performed to understand the interaction between NH_4^+ and bentonite. The effects of bentonite content and initial concentration on residual leachate concentration of Na^+ and NH_4^+ were investigated. The hydraulic conductivity coefficients of bentonite are obtained, and the SI of bentonite was tested. The relationship between swell potential and hydraulic conductivity coefficients of bentonite exposed to NaCl and NH_4Cl solution with different concentrations were analyzed.

2. METHODS

2.1. Materials

Geosynthetic clay liner (GCL) bentonite (abbr. bentonite) and natural clay obtained from Shanghai (abbr. clay) were used in this study. The main clay mineral of the bentonite is montmorillonite that accounts for 45.8% of clay mineral according to X-ray diffraction analyses. The basic physical properties of the bentonite and clay were tested as per ASTM D4318-10, as shown in Table 1. The bentonite is classified as a fat clay (CH).

NaCl and NH_4Cl solutions were prepared using analytically pure (AR99.5%) NaCl and NH_4Cl powders (analytical reagent, AR) obtained from Sinopharm Chemical Reagent Co., Ltd. Based on previous tests (Lou *et al.* 2007; Sun *et al.* 2021), the concentration of NH_4Cl solution is set at 9.4, 18.7, 37.4, and 74.8 mmol/L (It is equivalent to 500, 1,000, 2,000, and 4,000 mg/L respectively), corresponding to the residual NH_4^+ concentration after 2, 4, 6, and 8 years of operation in the landfill, respectively. It is reported that the concentrations of Na^+ were comparable to that of NH_4^+ in landfill leachate (Gupta & Paulraj 2017). Thus, the concentrations of NaCl were controlled to be equal to the concentrations of NH_4Cl.

2.2. Preparation of samples

The bentonite and clay were dried at 105 °C for 24 h. Subsequently, the dried bentonite was thoroughly mixed with dry clay powder to prepare a homogeneous dry mixture. The dry mixture comprised varying proportions of bentonite and clay, specifically 0, 5, 10, and 15%. Deionized water (DI water) was added to the dry mixture to achieve a mass ratio of water to dry mixture of 1:5. The mixture was rigorously mixed to ensure uniformity, and the resulting mixture samples were placed in

Table 1 | Basic physical indexes of bentonite and clay

Physical property	Bentonite	Natural clay
Liquid limit, w_L (%)	153.4	36.0
Plastic limit, w_p (%)	26.8	22.2
Plasticity index, (I_p)	126.6	13.8
Specific gravity (G_s)	2.7	2.7
Swelling index, *SI* (mL/2 g)	28.7	N.D.
Cation exchange capacity, *CEC* (meq/100 g)	68.0	N.D.
D_{50} (μm)	7.2	7.5
D_{97} (μm)	44.5	29.3

N.D., not determined.

sealed bags and left to stand for 24 h at 20 °C. Then, they were compacted using a jack to form samples with a diameter of 3.8 cm, a height of 1.5 cm, a specific gravity of 2.68 (±0.01) g/cm³, and a water content of 20% (±0.5%). In the saturated permeability test, the initial moisture content of the sample has modest influence on the test results, and the initial moisture content of 20% is set to make the soil sample reach a suitable plastic state in order prepare samples conveniently. This procedure was repeated to produce a total of 36 samples with varying bentonite contents. The samples used in the outflow measurement test are summarized as shown in Table 2.

2.3. Permeability test

The permeability test was conducted using an instrument of controlling water head pressure, as illustrated in Figure 1. Referring to the high hydraulic pressure tests (400 kPa) conducted by scholars such as Sun *et al.* 2021 and Chen *et al.* 2018 to shorten the testing time for low-permeability materials. The instrument is designed to create head pressure in the solution using air pressure.

Table 2 | The test scheme of outflow measurement

Type of solution	Dry density ρ_d (g/cm³)	Moisture content w (%)	Bentonite content a (%)	Concentration C (mmol/L)
DI water	1.7	20	0	/
			5	/
			10	/
			15	/
NaCl			0	9.4
			5	18.7
			10	37.4
			15	74.8
NH_4Cl			0	9.4
			5	18.7
			10	37.4
			15	74.8

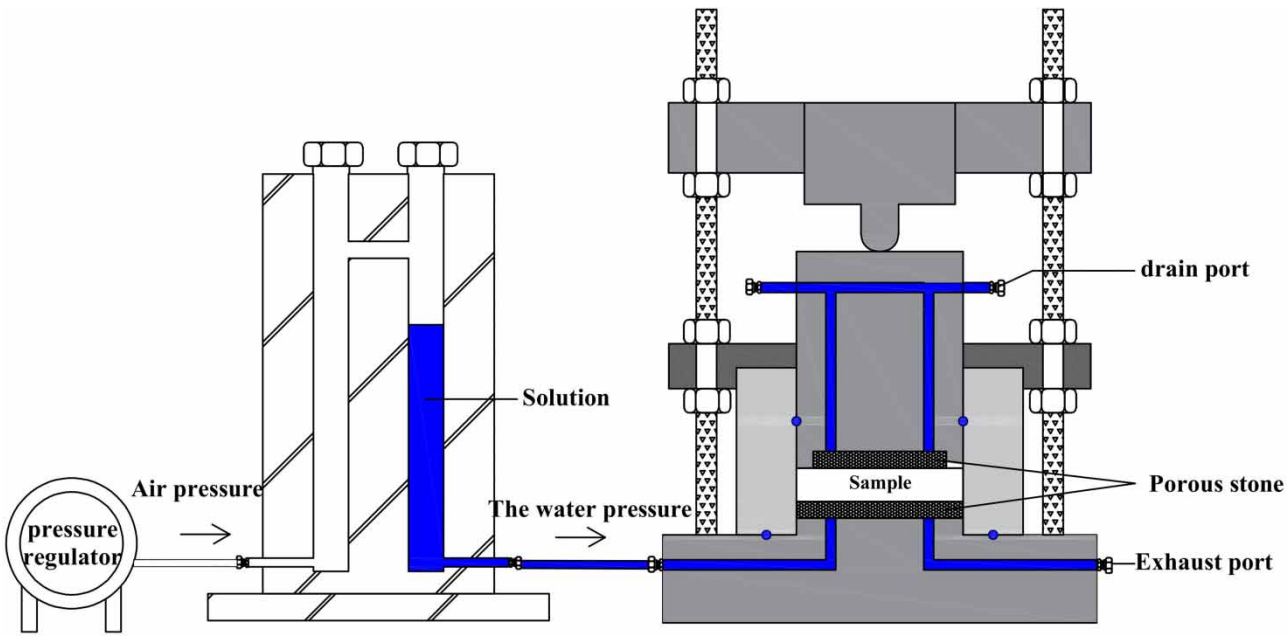

Figure 1 | Illustration of the constant head system.

The sample was installed on the instrument, with soaked filter papers and permeable stones placed at the upper and lower ends of the sample, respectively. Vaseline was applied to the inner walls of the instrument to ensure sealing. After fixing the sample in place, the appropriate permeation solution (NaCl or NH_4Cl) was introduced into the salt separator while ensuring the salt separator remained closed. Once the solution was added, the leachate collector was connected to the instrument. Subsequently, the air pressure valve was opened, and 400 kPa of air pressure was applied for a specified duration to remove any residual gas from the permeameter. During testing of each sample, the volume of the leachate found in the collector was continuously monitored and a relationship between time (s) and leachate volume (cm^3) can be obtained. When the leachate volume change rate becomes stable, it is considered that the sample has reached saturation and the permeability has reached a stable state. Finally, the permeation flux Q (cm^3/s) through the stable stage can be obtained and the hydraulic conductivity coefficient of the sample can be determined by Equation (1).

$$k = \frac{QL}{A\Delta h} \tag{1}$$

where k is the permeation coefficient of the sample; Q is the stable permeation flux (cm^3/s); L is the height of the sample (cm); A is the bottom area of the soil sample (cm^2); Δh is the hydraulic head difference (cm).

When the rate of change in permeation flux Q for three consecutive measurements is less than 1%, it is considered that permeation has reached equilibrium, and the permeability coefficient of the sample is obtained.

2.4. The residual leachate concentration tests

After obtaining stable hydraulic conductivity coefficients in the permeation tests described in Section 2.3, the leachate was obtained. The Na^+ concentration in the leachate was determined through Inductively Coupled Plasma (ICP) testing. The NH_4^+ concentration in the leachate was determined through Ion Chromatography (IC) testing.

2.5. SI test

Bentonite exhibits sensitive swelling behavior in cationic solutions. To conduct targeted research, the SI of bentonite was tested following ASTM D5890 standards. This test aimed to assess how the swelling potential of bentonite changes with varying Na^+/NH_4^+ concentrations. Each sample was tested in duplicate. The test scheme of SI is presented in Table 3. DI water was also used for comparative purposes.

Following the procedure outlined in ASTM D5890, not more than 0.1 g increments of bentonite were removed and were evenly distributed over the water surface in a graduated cylinder within a span of approximately 30 s. Additional bentonite was added continuously at 10-min intervals, ensuring that each increment swells without entrapping air between them, until the entire bentonite sample has been added. The bentonite sample was allowed to settle for 24 h from the last addition, and the volume level in mL was recorded to the nearest 0.5 mL at the top of the settled clay mineral.

2.6. FTIR analysis

FTIR analysis was applied to identify specific functional groups in the mixture samples containing NaCl and NH_4Cl solutions with concentration of 37.4 mmol/L and DIW. Fourier infrared spectrometer Nicolet6700 was used to record the spectra ranging from 4,000 to 400 cm^{-1} at a spectral resolution of 4 cm^{-1}. Scan repetition was 32 times. The sample used for FTIR analysis was prepared by mixing sample with KBr with a mass ratio of approximately 1–50. The sample name, bentonite content, type of solutions as well as its concentration are summarized in Table 4.

Table 3 | The test scheme of SI

Bentonite content (%)	Bentonite mass (g)	Type of solution	Concentration *C* (mmol/L)
5	1.45	NaCl	0
10	2.89	NH_4Cl	9.4
15	4.34		18.7
			37.4
			74.8

Table 4 | The test scheme of FTIR

Samples name	Bentonite content, α (%)	Type of solution	Concentration, C (mmol/L)
Na-sample	5	NaCl	37.4
NH_4-sample	5	NH_4Cl	37.4
DIW-sample	5	DIW	–

3. RESULTS

3.1. The residual leachate concentration of Na^+/ NH_4^+

Figure 2(a)–2(d) shows the variations between Na^+/NH_4^+ concentration of leachate through the mixture sample and bentonite content when mixture samples were subjected to NaCl and NH_4Cl solutions with concentration of 9.4, 18.7, 37.4, 74.8 mmol/L, respectively.

The result indicates that the NH_4^+ concentrations in leachate significantly decrease with increasing bentonite content, indicating an effective containment of NH_4^+ in leachate. The reduction in the concentration can be as high as 99% compared with

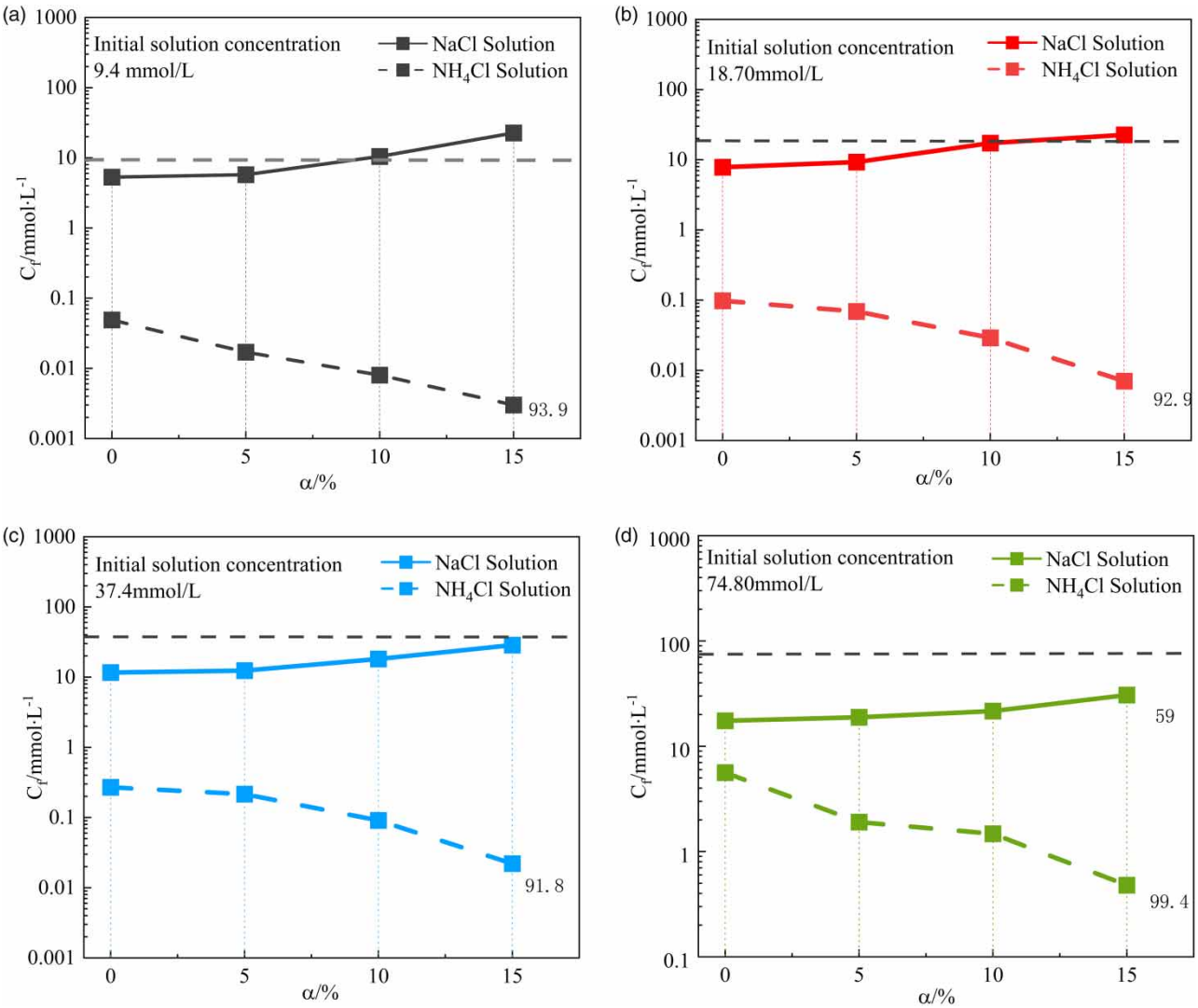

Figure 2 | Variations of the concentration of Na^+/NH_4^+ in leachate over bentonite contents under leachate of NaCl and NH_4Cl solutions. (a) $C = 9.4$ mmol/L, (b) $C = 18.7$ mmol/L, (c) $C = 37.4$ mmol/L, (d) $C = 74.8$ mmol/L.

its corresponding initial concentration. For example, as the bentonite content increases from 0 to 15%, the NH_4^+ concentrations in leachate decreases from 5.61 to 0.48 mmol/L when mixture samples subjected to NH_4Cl solution with initial concentration of 74.8 mmol/L.

In contrast, the variation in Na^+ concentration in leachate with bentonite content shows an opposite trend. The Na^+ concentration in leachate increases with an increase in bentonite content. It should be noted that the Na^+ concentration in leachate exceeds its initial concentration for mixture samples containing 15% bentonite, permeated with NaCl solutions initially at 9.4 and 18.7 mmol/L, as shown in Figure 2(a) and 2(b). The concentrations increase to 22.58 and 22.6 mmol/L, respectively. In addition, it is found that Na^+ concentration in leachate is generally higher than NH_4^+ concentration for a given bentonite content.

3.2. Permeability characteristics of bentonite in NaCl solution and NH_4Cl solution

The relationship between the hydraulic conductivity coefficient of mixed soil samples and the bentonite content at different Na^+/NH_4^+ concentrations is shown in Figure 3. As seen from the figure, the mixed soil samples exhibit the lowest hydraulic conductivity coefficient at a concentration of 0 mmol/L (DI water), and the hydraulic conductivity coefficient increases with the concentration of NaCl and NH_4Cl solutions. Notably, the mixed soil demonstrates different hydraulic conductivity characteristics in NaCl and NH_4Cl solutions, with the hydraulic conductivity coefficient generally being higher in NH_4Cl solutions than in NaCl solutions. In mixed soil samples with 5% bentonite content, this difference reaches up to 1.5 times (at a solution concentration of 74.8 mmol/L). Additionally, pure clay shows the highest hydraulic conductivity coefficient in deionized water, and as the bentonite content increases, the hydraulic conductivity coefficient of the mixed soil samples decreases from 11.2×10^{-9} cm/s to 1.1×10^{-9} cm/s. This trend is observed in both NaCl and NH_4Cl solutions.

3.3. SI of bentonite on NaCl solution and NH_4Cl solution

The SI refers to the increase in the volume of 2 g bentonite due to water absorption without applying any confined pressure (Dutta & Mishra 2015). It not only reflects the swelling potential but also the permeability and diffusion of metals (Chen *et al.* 2018). Figure 4 illustrates the relationship between the SI and bentonite masses at different Na^+/NH_4^+ concentration. The swelling of bentonite is not inhibited in DI water, with a SI of 31 mL/2 g. Compared to the 2.89 and 4.34 g samples of bentonite, the 1.45 g sample exhibits the highest level of free swelling. This trend remains consistent across solutions with different concentrations. Thereafter, the bentonite sample exhibits lower value of SI as the mass increases. The SI decreases with increasing Na^+/NH_4^+ concentration. In 1.45 g of bentonite, as the concentration of NaCl solution increases from 9.4 to 74.8 mmol/L, the SI decreases from 27.6 mL/2 g to 22.1 mL/2 g. Similarly, as the concentration of NH_4Cl solution increases

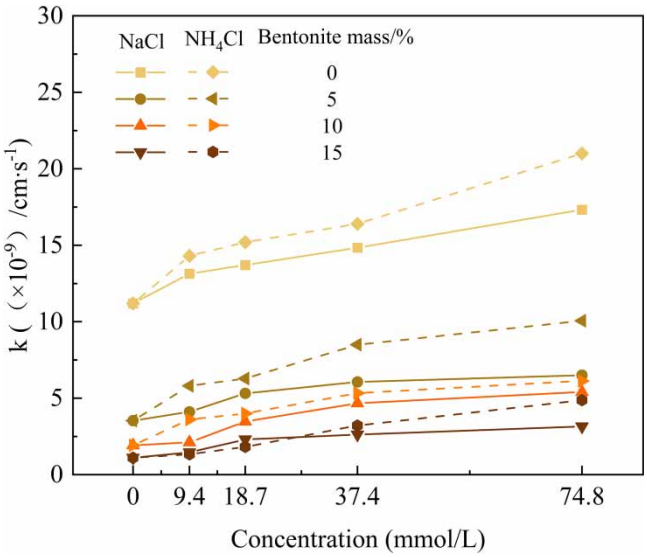

Figure 3 | Relationship between bentonite hydraulic conductivity coefficient and bentonite masses at different Na^+/NH_4^+ concentrations.

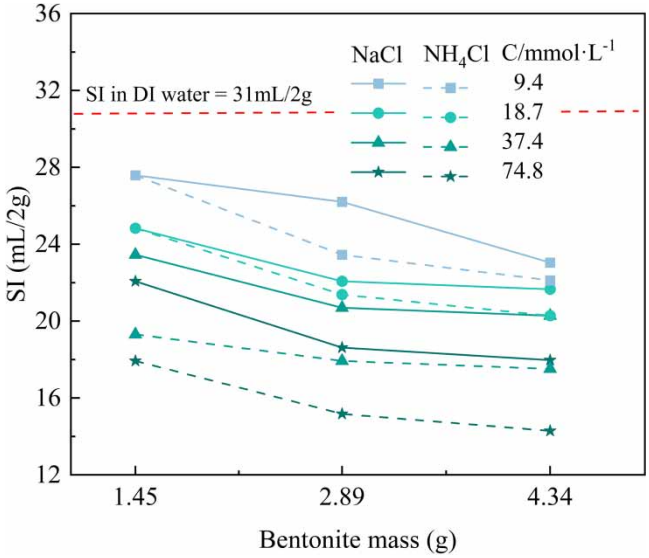

Figure 4 | Relationship between the SI and bentonite masses at different Na^+/NH_4^+ concentration.

from 9.4 to 74.8 mmol/L, the SI decreases from 27.6 mL/2 g to 17.9 mL/2 g. Bentonite exhibits differential swelling behavior in NaCl and NH_4Cl solutions, with lower free swelling observed in NH_4Cl solution.

3.4. FTIR

Figure 5 shows the resulting FTIR spectra of mixture samples with bentonite content of 5% exposed to DIW, and NaCl and NH_4Cl solution with concentration of 37.4 mmol/L. In addition, the specific bands of FTIR spectra are summarized in Table 5.

As shown in Figure 5, the band positions at 3,625 and 3,436 cm^{-1} are due to O–H vibration of cationic binding to octahedron and H–O–H vibration of montmorillonite surface absorbing water, respectively (Kumar & Lingfa 2020). The bands at 1,086 and 1,033 cm^{-1} are due to Si–O stretching vibration. The bands at 695–471 cm^{-1} are assigned to Si–O–Al bending vibration.

The band at 1,434 cm^{-1} is due to CO_3^{2-} entrainment in the mixture sample (Petit *et al.* 2006). The band offsets to 1,428 cm^{-1} after exposed to NH_4Cl solution is because the NH_4^+ bending vibration at 1,427 cm^{-1} (Gautier *et al.* 2010), indicating that NH_4^+ is fixed on montmorillonite.

In addition, two bands at 2,963 and 1,263 cm^{-1} are identified, as shown in Figure 6(a) and 6(b). These bands are located in the NH_4^+ stretching vibration region (3,300–2,800 cm^{-1}) and the NH_4^+ bending vibration region (1,700–700 cm^{-1}), respectively (Gautier *et al.* 2010). Compared to the FTIR spectra of samples in DI water and NaCl solution, new spectral bands appeared in the FTIR spectra of samples in NH_4Cl solution. This is attributed to the interaction between NH_4^+ and montmorillonite.

4. DISCUSSION

In the residual leachate concentration tests, the concentration of NH_4^+ was significantly lower than that of Na^+ (as discussed in Figure 2). The decrease in NH_4^+ concentration of leachate is attributed to the cation exchange between the pollutants and bentonite. The method of ion exchange has been used to remove metals from aqueous solutions (Hussain & Ali 2021). The interlayer cations in the montmorillonite mainly consist Na^+, K^+, Ca^{2+} and Mg^{2+} (Sun *et al.* 2013). It is reported that the cation replaceability order of bentonite can be as follows: $NH_4^+ > Ca^{2+} > Mg^{2+} > K^+ > Na^+$ (Ye *et al.* 2017; Xiang *et al.* 2020). This indicates that NH_4^+ in leachate can be fixed more easily due to exchange cation than Na^+.

Second, the hydration radius of NH_4^+ (5.35 Å) is smaller than that of Na^+ (7.9 Å) (Peng *et al.* 2018). This results in a closer fixture of NH_4^+ on negatively charged mineral surface than that of Na^+ (Helle *et al.* 2019). In addition, such hydration radius

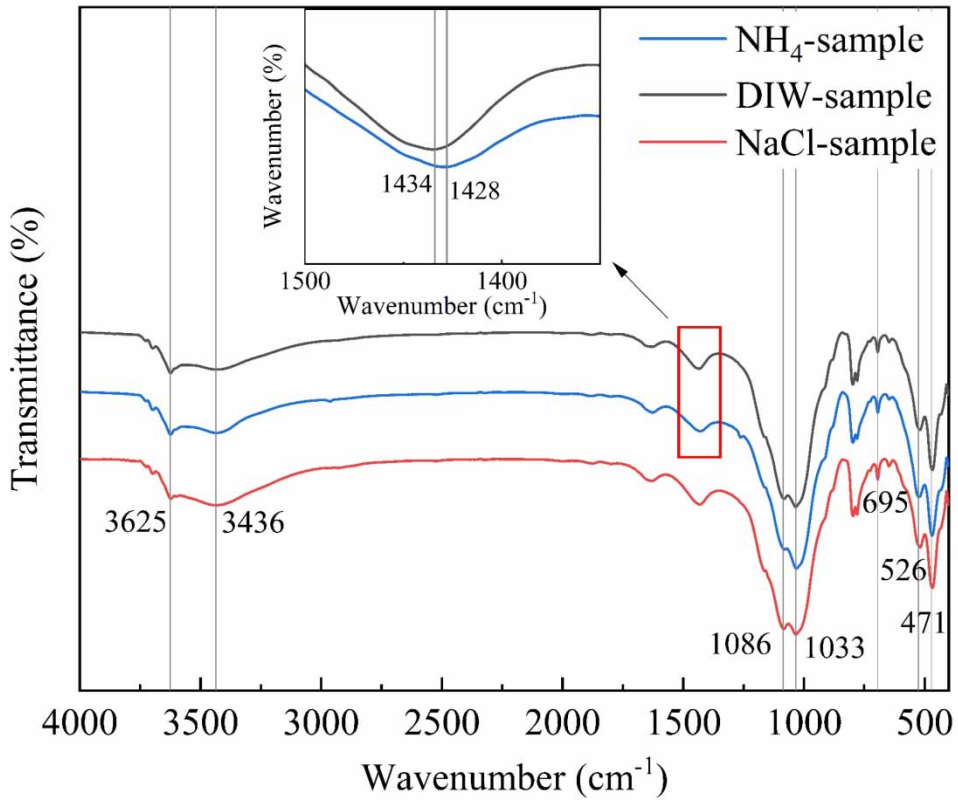

Figure 5 | FTIR spectra of DIW-sample, Na-sample, NH_4-sample.

Table 5 | Band location and assignment of FTIR spectrum

Assignment	Band location, (cm^{-1})	Reference
Symmetrical and asymmetrical O–H bond stretching vibrations of water	3,600–3,200	Gautier *et al.* (2010), Kumar & Lingfa (2020)
NH_4^+ stretching vibration	3,300–2,800	Gautier *et al.* (2010), Petit *et al.* (2006), Gautier *et al.* (2010)
NH_4^+ bending vibration	1,700–700	
Stretching vibration of Si–O	1,200–900	Zazoua *et al.* (2013)
Bending vibration of Al–O–Si	695.21–471.03	Hussain & Ali (2021)

of NH_4^+ allows NH_4^+ to be embedded into the hexatomic ring of silicon–oxygen tetrahedron, which can concatenate the clay layer by hydrogen bonds (N–H...O) between NH_4^+ and silicon hydroxyl groups (Zhang *et al.* 2020). Thus, the NH_4^+ can also be absorbed in inner-sphere complexes above the surface hexagonal cavities, as shown in Figure 7. Therefore, bentonite barriers exhibit good performance in intercepting NH_4^+. Notably, the Na^+ concentration in leachate increased compared to the initial concentration when a 9.4 mmol/L solution permeated the sample containing 15% bentonite (as seen in Figure 2). This is because the sodium-modified bentonite undergoes a chemical reaction where Na^+ replace Ca^{2+}, resulting in some Na^+ occupying the positions of Ca^{2+} (Sun *et al.* 2015). Unlike in sodium bentonite, these Na^+ diffuse into the NaCl solution driven by the concentration gradient. In this scenario, the concentration of Na^+ in the effluent may be higher than its initial concentration in the leachate.

The increase in hydraulic conductivity coefficient is due to the reduction in the double-layer thickness of montmorillonite particles caused by Na^+ and NH_4^+. Positively charged cations appear between the montmorillonite layers, weakening the

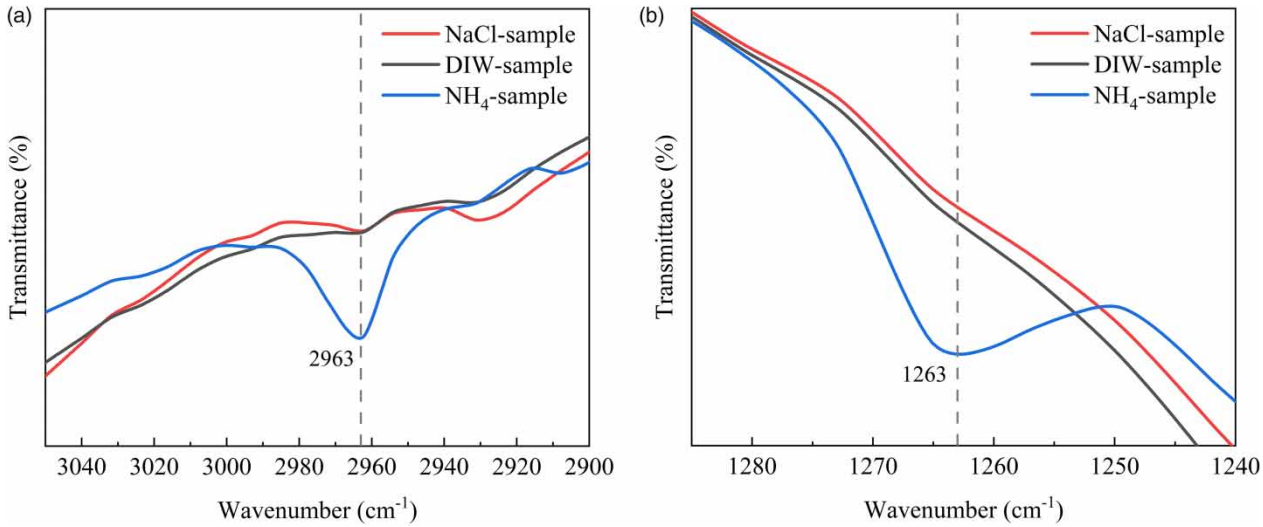

Figure 6 | FTIR spectra of band at 2,963 cm^{-1} (a) and 1,263 cm^{-1} (b).

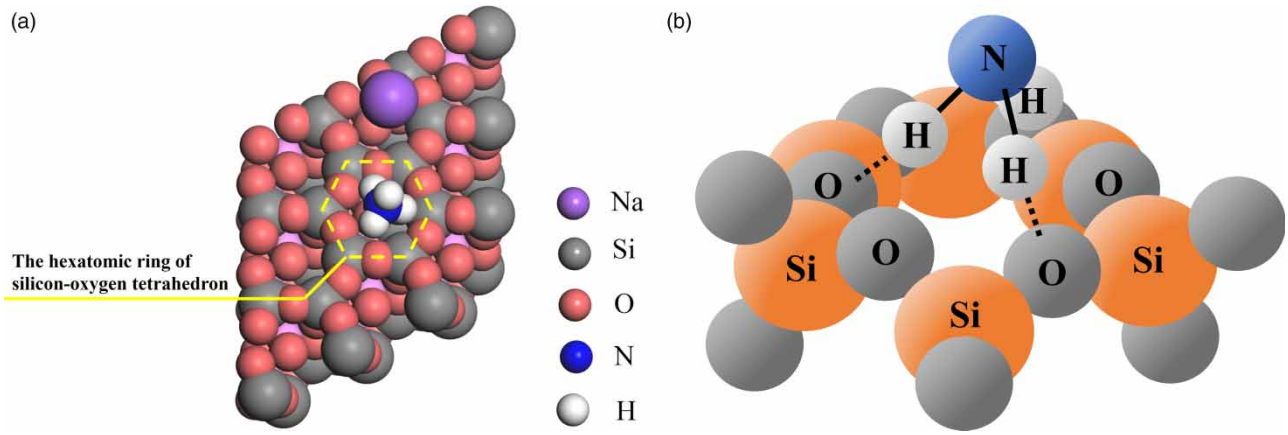

Figure 7 | Molecular model of NH_4^+ embedded in the hexatomic ring (a), and schematic representation of concatenate the layers by the hydrogen bonds (b) after Casal *et al.* (1984).

repulsion between the layers and the negative charges. This causes the microstructure to transition from a dispersed state to an aggregated state, leading to layer compression (Akinwunmi *et al.* 2020). It leads to an increase in the gaps between particles, reducing water flow resistance, and consequently increasing the hydraulic conductivity. The experimental results of the SI in Section 3.3 also support this view.

In this study, the SI of the mixture sample exposed to both NaCl and NH_4Cl solutions should theoretically be similar for a given concentration, as both Na^+ and NH_4^+ are monovalent cations. However, noticeable differences were observed, as shown in Figure 4. The lower SI of the mixture sample exposed to NH_4Cl solution is attributed to the lower hydration enthalpy of NH_4^+ compared to that of Na^+ (Peng *et al.* 2020; Morida *et al.* 2023). Hydration enthalpy serves as a measure of the interaction strength between a cation and water. Bentonite typically exhibits smaller swelling deformation in solutions with cations that have lower hydration enthalpy (Xiang *et al.* 2020). This results in differences in the swelling of bentonite in NaCl and NH_4Cl solutions. This indicates that the bentonite barrier may experience increased leachate percolation in NH_4Cl solution, potentially posing a risk of leakage for contaminants not adsorbed by the bentonite.

5. CONCLUSIONS

Permeation tests, concentration analysis, SI tests, and FTIR spectroscopy analysis were conducted to understand the pollutant interception and permeation characteristics of bentonite–natural clay mixtures in NaCl and NH_4Cl solutions. It can be concluded from the following points.

(1) The NH_4^+ concentrations in leachate significantly decrease with increasing bentonite content. The reduction in the concentration can be as high as 99% compared with NH_4^+ initial concentration, indicating an effective containment of NH_4^+ in leachate. In the residual leachate concentration, the Na^+ concentration is higher than the NH_4^+ concentration, with the difference reaching up to 1,000 times at certain points. The results indicate that the bentonite–clay mixture intercepts NH_4^+ more effectively than Na^+.

(2) The hydraulic conductivity coefficient of mixed soil samples increases with the concentration of NaCl and NH_4Cl solutions. The mixed soil samples demonstrate different hydraulic conductivity characteristics in NaCl and NH_4Cl solutions. Compared to NaCl solution, the samples have a lower SI and a higher hydraulic conductivity coefficient in NH4Cl solution. When a solution with a concentration of 74.8 mmol/L was used to permeate a mixed sample with 5% bentonite content, the difference in permeability coefficient reached 1.5 times.

(3) NH_4^+ is more readily intercepted in the interlayers of montmorillonite through cation exchange than Na^+. Additionally, the smaller hydration radius of NH_4^+ and the formation of hydrogen bonds contribute to the lower concentration of NH_4^+ compared to Na^+ in the leachate. This indicates that the bentonite barrier exhibits better interception of NH_4^+.

(4) The variation in hydraulic conductivity coefficient can be explained by the double-layer theory. Positively charged cations weaken the repulsion between the negative charges in the layers, causing layer compression. This leads to an increase in the gaps between particles, consequently increasing the hydraulic conductivity of the samples. NH_4^+ has a lower hydration enthalpy than Na^+, and bentonite typically exhibits smaller swelling deformation in solutions with cations of lower hydration enthalpy. This results in differences in the hydraulic conductivity coefficient of the samples in NaCl and NH_4Cl solutions.

ACKNOWLEDGEMENTS

We acknowledge the constructive feedback and suggestions provided by our colleagues and professionals, which helped improve the quality of this manuscript.

FUNDING

This research was financially supported by the National Natural Science Foundation of China (Grant No. 42372308, 51908121), the Natural Science Foundation of Shanghai Province (No. 22ZR1401800), and the Fundamental Research Funds for the Central Universities (No. 2232024A-06), the Open Funds of Hubei Key Laboratory of Disaster Prevention and Mitigation (No. 2022KJZ01) and the Open Funds of Engineering Research Center of Eco environment in Three Gorges Reservoir Region, Ministry of Education (No. KF2023–06).

ETHICS STATEMENT

Free and informed consent of the participants or their legal representatives was obtained and the study protocol was approved by the Donghua University.

DATA AVAILABILITY STATEMENT

Data cannot be made publicly available; readers should contact the corresponding author for details.

CONFLICT OF INTEREST

The authors declare there is no conflict.

REFERENCES

Akinwunmi, B., Hirvi, J. T., Kasa, S. & Pakkanen, T. A. 2020 Swelling pressure of Na- and Ca-montmorillonites in saline environments: A molecular dynamics study. *Chemical Physics* **528**, 110511. https://doi.org/10.1016/j.chemphys.2019.110511.

Anh, H. N., Ahn, H., Jo, H. Y. & Kim, G. Y. 2017 Effect of alkaline solutions on bentonite properties. *Environmental Earth Sciences* **76**, 374. https://doi.org/10.1007/s12665-017-6704-8.

Aryal, D. & Ganesan, V. 2018 Diffusivity of mono-and divalent salts and water in polyelectrolyte desalination membranes. *The Journal of Physical Chemistry B* **122** (33), 8098–8110. https://doi.org/10.1021/acs.jpcb.8b05979.

Casal, B., Ruiz-Hitzky, E. & Serratosa, J. M. 1984 Vibrational spectra of ammonium ions in crown-ether-NH_4^+-montmorillonite complexes. *Journal of the Chemical Society, Faraday Transactions 1: Physical Chemistry in Condensed Phases* **80**, 2225–2232. https://doi.org/10.1039/F19848002225.

Chen, J. N., Benson, C. H. & Edil, T. B. 2018 Hydraulic conductivity of geosynthetic clay liners with sodium bentonite to coal combustion product leachates. *Journal of Geotechnical and Geoenvironmental Engineering* **144** (4), 04018008. https://doi.org/10.1061/(ASCE)GT.1943-5606.0001844.

Costa, A. M., Alfaia, R. G. D. S. M. & Campos, J. C. 2019 Landfill leachate treatment in Brazil – an overview. *Journal of Environmental Management* **232**, 110–116. https://doi.org/10.1016/j.jenvman.2018.11.006.

Dong, T., Yao, J., Wang, Y., Luo, T. & Han, L. 2020 On the permselectivity of di-and mono-valent cations: Influence of applied current density and ionic species concentration. *Desalination* **488**, 114521. https://doi.org/10.1016/j.desal.2020.114521.

Dutta, J. & Mishra, A. K. 2015 A study on the influence of inorganic salts on the behaviour of compacted bentonites. *Applied Clay Science* **116-117**, 85–92. http://dx.doi.org/10.1016/j.clay.2015.08.018.

Gautier, M., Muller, F., Forestier, L. L., Beny, J. M. & Guegan, R. 2010 NH_4^+-smectite: characterization, hydration properties and hydro mechanical behaviour. *Applied Clay Science* **49**, 247–254. http://dx.doi.org/10.1016/j.clay.2010.05.013.

Gupta, A. & Paulraj, R. 2017 Leachate composition and toxicity assessment: An integrated approach correlating physicochemical parameters and toxicity of leachates from MSW landfill in Delhi. *Environmental Technology* **38**, 1599–1605. http://dx.doi.org/10.1080/09593330.2016.1238515.

Havukainen, J., Zhan, M., Dong, J., Liikanen, M., Deviatkin, I., Li, X. D. & Horttanainen, M. 2017 Environmental impact assessment of municipal solid waste management incorporating mechanical treatment of waste and incineration in Hangzhou, China. *Journal of Cleaner Production* **141**, 453–461. http://dx.doi.org/10.1016/j.jclepro.2016.09.146.

Helle, T. E., Aagaard, P., Nordal, S., Long, M. & Bazin, S. 2019 A geochemical, mineralogical and geotechnical characterization of the low plastic, highly sensitive glaciomarine clay at Dragvoll, Norway. *AIMS Geosciences* **5**, 704–722. https://doi.org/10.3934/geosci.2019.4.704.

Huang, D., Song, B. Y., He, Y. L., Ren, Q. L. & Yao, S. 2017 Cations diffusion in nafion117 membrane of microbial fuel cells. *Electrochimica Acta* **245**, 654–663. http://dx.doi.org/10.1016/j.electacta.2017.06.004.

Hussain, S. & Ali, S. 2021 Removal of heavy metal by ion exchange using bentonite clay. *Journal of Ecological Engineering* **22**, 104–111. https://doi.org/10.12911/22998993/128865.

Kumar, A. & Lingfa, P. 2020 Physicochemical characterization of sodium bentonite clay and its significance as a catalyst in plastic wastes valorization. *American Journal of Electronics & Communication* **1**, 6–9. https://doi.org/10.15864/ajec.1202.

Lai, H. J., Ding, X. Z., Cui, M. J., Zheng, J. J., Chen, Z. B., Pei, J. L. & Zhang, J. W. 2023 Mechanisms and influencing factors of biomineralization based heavy metal remediation: A review. *Biogeotechnics* **1** (3), 100039. https://doi.org/10.1016/j.bgtech.2023.100039.

Lou, Z. Y., Chai, X. L., Zhao, Y. C., Song, Y., Li, X. & Liu, Z. Y. 2007 Leachate compostion changes over time: Data from the laogang landfill in Shanghai. *Acta Scientiae Circumstantiae* **27** (6), 987–992. https://doi.org/0.13671/j.hjkxxb.2007.06.014.

Luo, H., Zeng, Y., Cheng, Y., He, D. & Pan, X. 2020 Recent advances in municipal landfill leachate: A review focusing on its characteristics, treatment, and toxicity assessment. *Science of the Total Environment* **703**, 135468. https://doi.org/10.1016/j.scitotenv.2019.135468.

Morida, K., Fukushi, K., Sakuma, H. & Tamura, K. 2023 Systematic comparison of the hydration and dehydration of Na^+-, K^+-, and NH_4^+-saturated montmorillonite, nontronite, hectorite, saponite, and Fe-saponite by in situ X-ray diffraction measurements. *Applied Clay Science* **237**, 106898. https://doi.org/10.1016/j.clay.2023.106898.

Naveen, B. P., Mahapatra, D. M., Sitharam, T. G., Sivapullaiah, P. V. & Ramachandra, T. V. 2017 Physico-chemical and biological characterization of urban municipal landfill leachate. *Environmental Pollution* **220**, 1–12. http://dx.doi.org/10.1016/j.envpol.2016.09.002.

Negi, P., Mor, S. & Ravindra, K. 2020 Impact of landfill leachate on the groundwater quality in three cities of North India and health risk assessment. *Environment, Development and Sustainability* **22**, 1455–1474. https://doi.org/10.1007/s10668-018-0257-1.

Özçoban, M. Ş., Acarer, S. & Tüfekci, N. 2022 Effect of solid waste landfill leachate contaminants on hydraulic conductivity of landfill liners. *Water Science and Technology* **85** (5), 1581–1599. https://doi.org/10.2166/wst.2022.033.

Peng, J., Lou, K., Goenaga, G. & Zawodzinski, T. A. 2018 Transport properties of perfluorosulfonate membranes ion exchanged with cations. *ACS Applied Materials & Interfaces* **10** (44), 38418–38430. https://doi.org/10.1021/acsami.8b12403.

Peng, C., Wang, G., Qin, L., Luo, S., Min, F. & Zhu, X. 2020 Molecular dynamics simulation of NH_4-montmorillonite interlayer hydration: Structure, energetics, and dynamics. *Applied Clay Science* **195**, 105657. https://doi.org/10.1016/j.clay.2020.105657.

Petit, S., Righi, D. & Madejová, J. 2006 Infrared spectroscopy of NH_4^+-bearing and saturated clay minerals: A review of the study of layer charge. *Applied Clay Science* **34**, 22–30. https://doi.org/10.1016/j.clay.2006.02.007.

Setz, M. C., Tian, K., Benson, C. H. & Bradshaw, S. L. 2017 Effect of ammonium on the hydraulic conductivity of geosynthetic clay liners. *Geotextiles and Geomembranes* **45**, 665–673. http://dx.doi.org/10.1016/j.geotexmem.2017.08.008.

Sun, D. A., Zhang, J. Y., Zhang, J. R. & Zhang, L. 2013 Swelling characteristics of GMZ bentonite and its mixtures with sand. *Applied Clay Science* **83–84**, 224–230. https://doi.org/10.1016/j.clay.2013.08.042.

Sun, D. A., Zhang, L., Li, J. & Zhang, B. C. 2015 Evaluation and prediction of the swelling pressures of GMZ bentonites saturated with saline solution. *Applied Clay Science* **105**, 207–216. https://doi.org/10.1016/j.clay.2014.12.032.

Sun, W. J., Xu, G., Wei, G., Zhang, W. J. & Sun, D. A. 2021 Effects of ammonium ion and bentonite content on permeability of bentonite-clay mixture. *Environmental Earth Sciences* **80**, 151. https://doi.org/10.1007/s12665-021-09440-w.

Tadimeti, J. G. D. & Chattopadhyay, S. 2016 Physico-chemical local equilibrium influencing cation transport in electrodialysis of multi-ionic solutions. *Desalination* **385**, 93–105. http://dx.doi.org/10.1016/j.desal.2016.02.016.

Xiang, G., Ye, W., Xu, Y. & Jalal, F. E. 2020 Swelling deformation of Na-bentonite in solutions containing different cations. *Engineering Geology* **277**, 105757. https://doi.org/10.1016/j.enggeo.2020.105757.

Ye, W. M., Zhang, F., Chen, Y. G., Chen, B. & Cui, Y. J. 2017 Influences of salt solutions and salinization-desalinization processes on the volume change of compacted GMZ01 bentonite. *Engineering Geology* **222**, 140–145. https://doi.org/10.1016/j.enggeo.2017.04.002.

Zazoua, A., Kazane, I., Khedimallah, N., Dernane, C., Errachid, A. & Jaffrezic-Renault, N. 2013 Evidence of ammonium ion-exchange properties of natural bentonite and application to ammonium detection. *Materials Science and Engineering: C* **33**, 5084–5089. http://dx.doi.org/10.1016/j.msec.2013.09.005.

Zhang, R., Wang, X., Sun, Y., Zhang, J., Hu, W., Du, W. & Chen, G. 2020 Preparation and performance of ammonium-malic salts as shale swelling inhibitor and a mechanism study. *Inorganic and Nano-Metal Chemistry* **50**, 1027–1031. http://dx.doi.org/10.1080/24701556.2020.1732418.

First received 8 March 2024; accepted in revised form 26 June 2024. Available online 16 July 2024